ISSN 1027-4510, Journal of Surface Investigation. X-ray, Synchrotron and Neutron Techniques, 2014, Vol. 8, No. 6, pp. 1351–1359. © Pleiades Publishing, Ltd., 2014.
Original Russian Text © S.V. Blazhevich, Yu.P. Gladkikh, A.V. Noskov, 2014, published in Poverkhnost'. Rentgenovskie, Sinkhrotronnye i Neitronnye Issledovaniya, 2014, No. 12, pp. 91–99.

Manifestation of the Effects of Dynamic Diffraction in the Coherent X-ray Radiation of Relativistic Electrons in a Periodic Layered Medium

S. V. Blazhevich, Yu. P. Gladkikh, and A. V. Noskov

National Research Belgorod State University, Belgorod, 308007 Russia

e-mail: noskovbupk@mail.ru

Received January 20, 2014

Abstract—The possibility of manifestation of the effects of dynamic diffraction in the coherent X-ray radiation of relativistic electrons in a periodic layered medium is studied theoretically in this paper.

DOI: 10.1134/S1027451014060251

INTRODUCTION

In the past, the radiation of relativistic particles in a periodic layered medium was regarded as resonant transition radiation (RTR) [1]. The first experimental and theoretical studies of RTR in periodic layered media were presented in [2–9]. The experimental works [7–9], in which RTR spectra were measured with great accuracy, agreed well with theoretical calculations. Beginning approximately in 1985, interest in RTR grew because of the possibility of its use as a new source of convertible coherent radiation in the range of keV-photon frequencies. A group of physicists in Japan made a large contribution to the study of RTR [10–12]. In [11], periodic media with plate thicknesses of several hundred nanometers were used for the first time, and the emitted photons at the first harmonics have frequencies of 2–4 keV; in this case, the authors stated that the attained intensity exceeded that of the synchrotron radiation of existing accelerators. Parametric radiation (PXR), together with RTR, was considered in [13]. It is necessary to note that various methods were used to describe the process of relativistic electron radiation in a periodic layered structure [14–20]; however, the authors of [21] were the first to consider radiation from a multilayer periodic layered structure in the dynamic approximation as the scattering of pseudophotons of the Coulomb field of relativistic electrons at amorphous layers by analogy with the process of coherent radiation produced by relativistic electrons in a crystalline medium. Coherent X-ray radiation in a periodic layered structure was regarded as the resultant effect of two mechanisms of radiation, namely, PXR and diffracted transition radiation (DTR). The dynamic theory of relativistic electron radiation in periodic layered media [21] well described the experimental data in [22], where layers of a structure with a thickness of about 1 nm were used and photons with a frequency of 15 keV were generated. We note that, in all cited papers [1–22], the process of emission in a periodic layered medium was regarded only in the Bragg scattering geometry in the case of symmetric reflection, where the angle between the surface and reflecting planes was zero and emitted photons escaped through the front target boundary. The authors of [23–25] developed the dynamic theory of the coherent X-ray radiation of relativistic electrons in periodic layered media in the general case of asymmetric reflection of the electron field with respect to the target surface, i.e., when reflecting target layers were located at a certain angle to the target surface.

In this paper, we consider the possibility and conditions for manifestation of the effects of dynamic diffraction in the coherent X-ray radiation of relativistic electrons passing through a periodic layered medium. The effects of dynamic diffraction are well-known in the physics of the scattering of free X rays in crystals [26], and their manifestation in the coherent radiation of relativistic electrons in crystals was studied in [27–31].

SPECTRAL AND ANGULAR DENSITIES OF THE COHERENT X-RAY RADIATION OF RELATIVISTIC ELECTRONS IN LAUE SCATTERING GEOMETRY

We consider the radiation of relativistic electrons passing through a periodic layered medium with the velocity $\mathbf{V}$ in Laue scattering geometry (Fig. 1); this medium consists of periodically located amorphous layers with thicknesses of a and b and with respective permittivities of χ_a and χ_b. The layered-structure period was $T = a + b$. In Fig. 1, $\boldsymbol{\mu} = \mathbf{k} - \omega\mathbf{V}/V^2$ is the component of the virtual-photon momentum that is perpendicular to the particle velocity $\mathbf{V}$ ($\mu = \omega\theta/V$, where $\theta \ll 1$ is the angle between the vectors $\mathbf{k}$ and $\mathbf{V}$),

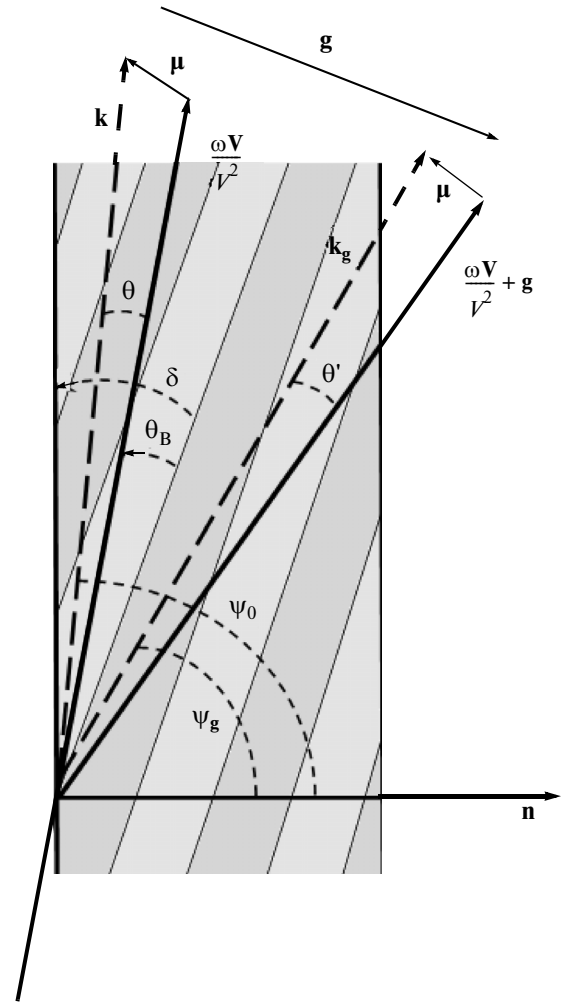

Fig. 1. Geometry of the emission process: θ and θ' are the emission angles, θ_B is the Bragg angle (the angle between the electron velocity **V** and the reflecting layers), δ is the angle between the surface and the target layers, and **k** and $\mathbf{k_g}$ are the wave vectors of the incident and diffracted photons.

θ_B is the Bragg angle, and φ is the azimuthal emission angle measured from the plane formed by the electron velocity vector **V** and the vector **g** that is perpendicular to the reflecting layers. The length of the vector **g** can be expressed in terms of the Bragg angle and the Bragg frequency ω_B: $g = 2\omega_B \sin\theta_B/V$. The vector **g** is analogous to the reciprocal-lattice vector in the crystal and is perpendicular to the structure layers; its length is $g = \frac{2\pi}{T}n$, $n = 0, \pm 1, \pm 2, \ldots$. Because the relativistic-particle field can be regarded as transverse, the incident $\mathbf{E}_0(\mathbf{k},\omega)$ and the diffracted $\mathbf{E}_\mathbf{g}(\mathbf{k},\omega)$ electromagnetic waves to which the respective wave vectors **k** and $\mathbf{k_g} = \mathbf{k} + \mathbf{g}$ correspond are determined by two amplitudes with different transverse polarizations:

$$\mathbf{E}_0(\mathbf{k},\omega) = E_0^{(1)}(\mathbf{k},\omega)\mathbf{e}_0^{(1)} + E_0^{(2)}(\mathbf{k},\omega)\mathbf{e}_0^{(2)},$$
$$\mathbf{E}_\mathbf{g}(\mathbf{k},\omega) = E_\mathbf{g}^{(1)}(\mathbf{k},\omega)\mathbf{e}_\mathbf{g}^{(1)} + E_\mathbf{g}^{(2)}(\mathbf{k},\omega)\mathbf{e}_\mathbf{g}^{(2)},$$

where vectors $\mathbf{e}_0^{(1)}$ and $\mathbf{e}_0^{(2)}$ are perpendicular to vector **k** and vectors $\mathbf{e}_\mathbf{g}^{(1)}$ and $\mathbf{e}_\mathbf{g}^{(2)}$ are perpendicular to vector $\mathbf{k_g}$. The vectors $\mathbf{e}_0^{(2)}$ and $\mathbf{e}_\mathbf{g}^{(2)}$ lie in the plane of vectors **k** and $\mathbf{k_g}$ (π polarization), and the vectors $\mathbf{e}_0^{(1)}$ and $\mathbf{e}_\mathbf{g}^{(1)}$ are perpendicular to it (σ polarization).

Within the framework of the two-wave approximation of dynamic diffraction theory, the authors of [23] obtained expressions describing the spectral and angular characteristics of radiation in the direction of vector $\mathbf{k_g}$, in which the coherent X-ray radiation of a relativistic electron moving in the rectilinear direction was represented as the sum of parametric X-ray radiation and diffracted transition radiation.

We write the expressions for the spectral and angular densities in the form

$$\omega\frac{d^2N_{\mathrm{PXR}}^{(s)}}{d\omega d\Omega} = \frac{e^2}{4\pi^2}P^{(s)^2} \times \frac{\theta^2}{\left(\theta^2 + \gamma^{-2} - (\chi_a' + r\chi_b')/(1+r)\right)^2}R_{\mathrm{PXR}}^{(s)}, \quad (1a)$$

$$R_{\mathrm{PXR}}^{(s)} = \left(1 - \frac{\xi}{\sqrt{\xi^2+\varepsilon}}\right)^2 \frac{1 + \exp\left(-L_f\mu_1^{(s)}\right) - 2\exp\left(-L_f\mu_1^{(s)}/2\right)\cos\left(\frac{L_e}{2L_{\mathrm{ext}}}\left(\sigma^{(s)} + \frac{\xi - \sqrt{\xi^2+\varepsilon}}{\varepsilon}\right)\right)}{\left(\sigma^{(s)} + \frac{\xi - \sqrt{\xi^2+\varepsilon}}{\varepsilon}\right)^2 + \left(\frac{\mu_1^{(s)}L_{\mathrm{ext}}}{\varepsilon}\right)^2}, \quad (1b)$$

$$\omega\frac{d^2N_{\mathrm{DTR}}^{(s)}}{d\omega d\Omega} = \frac{e^2}{4\pi^2}P^{(s)^2}\theta^2 \times \left(\frac{1}{\theta^2+\gamma^{-2}} - \frac{1}{\theta^2 + \gamma^{-2} - (\chi_a' + r\chi_b')/(1+r)}\right)^2 R_{\mathrm{DTR}}^{(s)}, \quad (2a)$$

$$R_{\mathrm{DTR}}^{(s)} = \frac{\varepsilon^2}{\xi(\omega)^2 + \varepsilon}\left[\exp\left(-L_f\mu_1^{(s)}\right) + \exp\left(-L_f\mu_2^{(s)}\right) - 2\exp\left(-L_f\mu_0\left(\frac{1+\varepsilon}{2}\right)\right)\cos\left(\frac{L_f}{L_{\mathrm{ext}}^{(s)}}\sqrt{\xi^2+\varepsilon}\right)\right]. \quad (2b)$$

The following notation was introduced in expressions (1) and (2):

$$\mu_1^{(s)} = \mu_0\left(\frac{1+\varepsilon}{2} - \frac{(1-\varepsilon)\xi^{(s)}(\omega) + 2\varepsilon\kappa^{(s)}}{2\sqrt{\xi^{(s)}(\omega)^2 + \varepsilon}}\right),$$

$$\mu_2^{(s)} = \mu_0\left(\frac{1+\varepsilon}{2} + \frac{(1-\varepsilon)\xi^{(s)}(\omega) + 2\varepsilon\kappa^{(s)}}{2\sqrt{\xi^{(s)}(\omega)^2 + \varepsilon}}\right),$$

$$\mu_0 = \omega\left(\frac{\left|r\chi_b'' + \chi_a''\right|}{1+r}\right),$$

$$L_\mathrm{f} = \frac{L}{\sin(\delta+\theta_\mathrm{B})}, \quad L_e = \frac{L}{\sin(\delta-\theta_\mathrm{B})},$$

$$L_{\mathrm{ext}}^{(s)} = \frac{1}{C^{(s)}\omega}\frac{\pi n}{\left|\sin\left(\frac{\pi n}{1+r}\right)\right|\left|\chi_b' - \chi_a'\right|}.$$

Expression (1) and (2) for the parameter $s = 1$ describe σ-polarized fields, and for $s = 2$ – π-polarized ones; in this case, $C^{(s)} = \mathbf{e}_0^{(s)}\mathbf{e}_1^{(s)}$, $C^{(1)} = 1$, $C^{(2)} = \cos 2\theta_\mathrm{B}$, $P^{(s)} = \mathbf{e}_0^{(s)}(\boldsymbol{\mu}/\mu)$, $P^{(1)} = \sin\varphi$, and $P^{(2)} = \cos\varphi$.

$$\kappa^{(s)} = \frac{C^{(s)}\left|\sin\left(\frac{\pi n}{1+r}\right)\right|}{\frac{\pi n}{1+r}}\left|\frac{\frac{\chi_b''}{\chi_a''} - 1}{r\frac{\chi_b''}{\chi_a''} + 1}\right|,$$

$$\sigma^{(s)} = \omega_\mathrm{B}L_{\mathrm{ext}}^{(s)}\left(\theta^2 + \gamma^{-2} + \frac{\left|r\chi_b' + \chi_a'\right|}{1+r}\right),$$

$$\xi^{(s)}(\omega) = \frac{1}{\nu^{(s)}}\left(2\sin^2\theta_\mathrm{B}\frac{1+r}{\left|\chi_a' + r\chi_b'\right|}\right. \tag{3}$$

$$\left.\times\left(1 - \frac{\omega(1-\theta\cos\varphi\cot\theta_\mathrm{B})}{\omega_\mathrm{B}}\right) + \frac{1-\varepsilon}{2}\right),$$

$$\varepsilon = \frac{\sin(\delta+\theta_\mathrm{B})}{\sin(\delta-\theta_\mathrm{B})}, \quad \nu^{(s)} = \frac{C^{(s)}\left|\sin\left(\frac{\pi n}{1+r}\right)\right|}{\frac{\pi n}{1+r}}\left|\frac{\frac{\chi_b'}{\chi_a'} - 1}{r\frac{\chi_b'}{\chi_a'} + 1}\right|,$$

$$r = \frac{b}{a},$$

where $\mu_1^{(s)}$ and $\mu_2^{(s)}$ are the dynamic effective absorption coefficients, L_f is the photon path in the target, L_e is the electron path in the target, $L_{\mathrm{ext}}^{(s)}$ is the extinction length for X-rays in the periodic layered medium, $\xi^{(s)}(\omega)$ is a spectral function rapidly varying with frequency, and ε is the parameter determining the degree of asymmetry of the electron-field reflection with respect to the target surface, and r is the parameter determining the ratio of the layer thicknesses in the target.

For clarity, in what follows, all numerical calculations are given for σ-polarized waves ($s = 1$) and the first harmonic of excited X-ray wave reflection.

DYNAMIC COEFFICIENTS OF X-RAY WAVE ABSORPTION IN A LAYERED MEDIUM

We consider the dynamic coefficients $\mu_1^{(s)}$ and $\mu_2^{(s)}$ of X-ray absorption in a periodic layered medium. We note that both of them contain the parameter μ_0, which is the linear coefficient of X-ray absorption in a layered medium in the kinematic approximation. The difference between $\mu_1^{(s)}$ and $\mu_2^{(s)}$ and μ_0 is determined by the interference and the mutual transfer of incident and diffracted waves, which in the dynamic approximation are regarded as equal. The difference between the absorption coefficients of two waves excited in the layered medium is determined by the second multiplier, which depends on the photon frequency and the target parameters:

$$\frac{\mu_{1,2}^{(s)}}{\mu_0} = \left(\frac{1+\varepsilon}{2} \mp \frac{(1-\varepsilon)\xi^{(s)}(\omega) + 2\varepsilon\kappa^{(s)}}{2\sqrt{\xi^{(s)}(\omega)^2 + \varepsilon}}\right). \tag{4}$$

The parameter $\kappa^{(s)}$ contained in the formulae for $\mu_1^{(s)}$ and $\mu_2^{(s)}$ determines the locations of antinodes of standing waves formed upon superposition of the incident and diffracted waves inside the layered structure. It can be seen that, as parameter $\kappa^{(s)}$ approaches 1, $\mu_1^{(s)}$ decreases and $\mu_2^{(s)}$ increases. In the case when $\kappa^{(s)} \approx 1$, the antinode maxima of one standing wave with the absorption coefficient $\mu_1^{(s)}$ are located in layers of the compound with a smaller electron density. The absorption of this wave is minimal, and the absorption of another wave with the absorption coefficient $\mu_2^{(s)}$ is maximal. This effect is well known in the physics of free X-ray scattering in crystals and is called the Borrmann effect. It can be seen from expression (3) for the parameter $\kappa^{(s)}$ that it depends on the ratio $r = \frac{b}{a}$ of the reflecting-layer thicknesses. As an example, we consider the dependence of the parameter $\kappa^{(s)}$ on b/a for a periodic layered medium consisting of a W layer with a thickness of b and a C layer with a thickness of a in the case of the emission of X-ray photons with a certain Bragg frequency ω_B. The dependence $\kappa^{(s)}$ on b/a shown in Fig. 2 is constructed for the first harmonics ($n = 1$) of σ polarized waves ($s = 1$). It can be seen from Fig. 2 that, as b/a decreases, the parameter $\kappa^{(s)}$ first increases and then decreases. When studying the

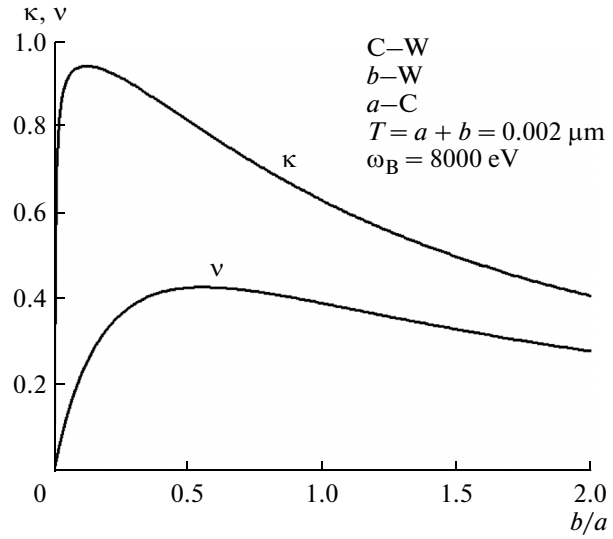

Fig. 2. Dependence of the parameters of dynamic X-ray scattering on the ratio of the thicknesses of layers of the emitting layered structure.

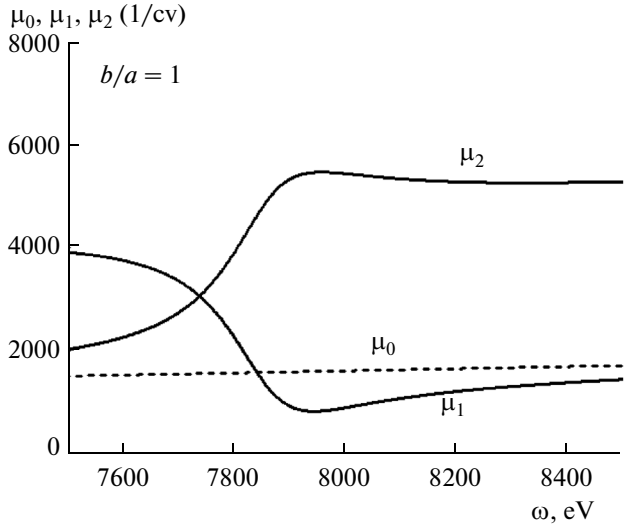

Fig. 3. Absorption coefficients for two X-ray waves in a layered structure. The curves are constructed under the condition $b/a \approx 1$.

coherent radiation of relativistic electrons, it is necessary also to take into account the dynamic scattering parameter $\nu^{(s)}$ ranging from 0 to 1 and determining the degree of field reflection from the periodic structure, which is due to the character of the interference of waves reflected from different planes, namely, constructive ($\nu^{(s)} \approx 1$) or destructive ($\nu^{(s)} \approx 0$). The expressions for the angular PXR and DTR densities following from (1) and (2) are proportional to the parameter $\nu^{(s)}$:

$$\frac{dN^{(s)}_{\mathrm{PXR}}}{d\Omega} = \nu^{(s)} \frac{e^2}{8\pi^2 \sin^2\theta_{\mathrm{B}}} \frac{\left|\chi'_a + r\chi'_b\right|}{1+r} \times \frac{P^{(s)^2}\theta^2}{\left(\theta^2 + \gamma^{-2} - (\chi'_a + r\chi'_b)/(1+r)\right)^2} \int_{-\infty}^{+\infty} R^{(s)}_{\mathrm{PXR}} d\xi^{(s)}(\omega), \quad (5)$$

$$\frac{dN^{(s)}_{\mathrm{DTR}}}{d\Omega} = \nu^{(s)} \frac{e^2}{8\pi^2 \sin^2\theta_{\mathrm{B}}} \frac{\left|\chi'_a + r\chi'_b\right|}{1+r} P^{(s)^2}\theta^2 \times \left(\frac{1}{\theta^2 + \gamma^{-2}} - \frac{1}{\theta^2 + \gamma^{-2} - (\chi'_a + r\chi'_b)/(1+r)}\right)^2 \times \int_{-\infty}^{+\infty} R^{(s)}_{\mathrm{DTR}} d\xi^{(s)}(\omega). \quad (6)$$

In the case of the approximate equality of the real parts of the permittivities ($\chi'_b \approx \chi'_a$) of the amorphous media constituting the periodic structure, the parameter $\nu^{(s)}$ is small; consequently, the radiation intensity is also small. It is obvious that in the limiting case where the thickness of any of the layers tends to zero ($a \to 0$ or $b \to 0$), the parameter $\nu^{(s)} \to 0$, and the medium becomes homogeneous. In this case, there are naturally no reflections, because there also is no periodic structure $\frac{dN^{(s)}}{d\Omega} = 0$.

The curve describing the dependence of the parameter $\nu^{(s)}$ on the ratio b/a is also given in Fig. 2. It can be seen that, for b/a corresponding to maximal $\kappa^{(s)}$, the parameter $\nu^{(s)}$ is small; i.e., the interference of the waves reflected from different planes has a destructive character. But in the case where $b/a \approx 0.25$, wave reflection is almost maximal, and parameter $\kappa^{(s)}$ is still large so that it can provide a decrease in the absorption of one of the waves and the corresponding manifestation of the dynamic effect of anomalous absorption (the Borrmann effect) for PXR and DTR in the periodic layered medium. Thus, from the consideration of the effective coefficients of X-ray absorption, it can be concluded that the anomalous absorption of one of the excited fields ($\mu_2^{(s)} > \mu_0$) and the anomalous propagation of X rays of the second field ($\mu_1^{(s)} \ll \mu_0$) occur in the case of the dynamic scattering of X rays in an absorbing periodic medium (Fig. 3). As the parameter $\kappa^{(s)}$ increases, because of an increase in the ratio of the thicknesses of the reflecting layers up to $b/a \approx 0.25$, in the neighborhood of the Bragg frequency, the absorption of one of the waves increases and that of the other decreases (Fig. 4); i.e., the Borrmann effect increases.

MANIFESTATION OF THE EFFECTS OF DYNAMIC DIFFRACTION IN RADIATION

We consider the spectral and angular characteristics of DTR, which is a consequence of diffraction (at

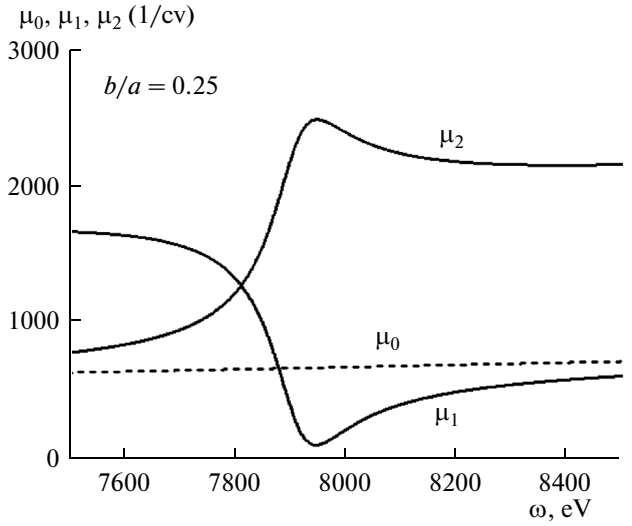

Fig. 4. Absorption coefficients for two X-ray waves in a layered structure. The curves are constructed under the condition $b/a \approx 0.25$, at which the Borrmann effect is manifested.

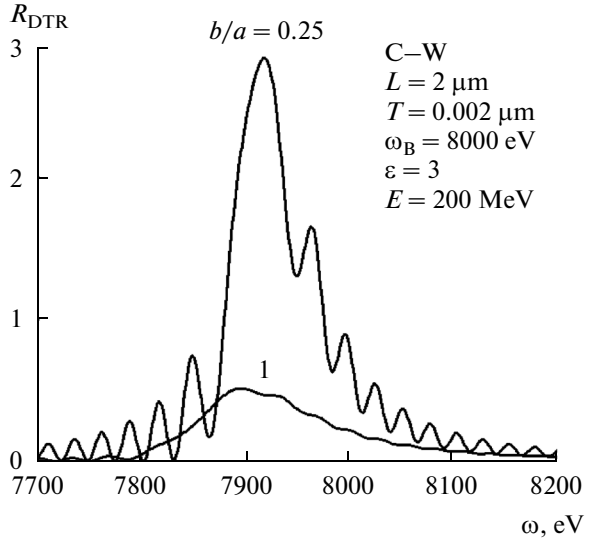

Fig. 5. DTR spectrum under the condition of clear manifestation of the Borrmann effect $b/a \approx 0.25$ and in the case $b/a \approx 1$.

target layers) of transition radiation produced when relativistic electrons cross the front target boundary. Figure 5 shows curves describing the spectral DTR density of a relativistic electron with an energy of $E =$ 200 MeV generated in the C–W target; these curves were constructed using formula (2) for two different values of the ratio b/a of the layer thicknesses and for values of other parameters given in the figure. It can be seen that the spectral amplitude under condition $b/a \approx 0.25$ ($\kappa^{(s)} \approx 1$) significantly exceeds that under condition $b/a \approx 1$ ($\kappa^{(s)} \approx 0.3$) (Fig. 2), which is related to a stronger manifestation of the Borrmann effect in the first case.

We consider the contribution of each of the two excited DTR waves and their interference in the total spectrum under the condition of Borrmann effect manifestation. For this purpose, we represent expression (2) in the form

$$R_{\mathrm{DTR}}^{(s)} = R_1^{(s)} + R_2^{(s)} + R_{\mathrm{INT}}^{(s)}, \tag{7a}$$

$$R_1^{(s)} = \frac{\varepsilon^2}{\xi(\omega)^2 + \varepsilon} \exp\left(-L_{\mathrm{f}}\mu_1^{(s)}\right), \tag{7b}$$

$$R_2^{(s)} = \frac{\varepsilon^2}{\xi(\omega)^2 + \varepsilon} \exp\left(-L_{\mathrm{f}}\mu_2^{(s)}\right), \tag{7c}$$

$$R_{\mathrm{INT}}^{(s)} = -2\frac{\varepsilon^2}{\xi(\omega)^2 + \varepsilon} \times \exp\left(-L_{\mathrm{f}}\mu_0\left(\frac{1+\varepsilon}{2}\right)\right)\cos\left(\frac{L_{\mathrm{f}}}{L_{\mathrm{ext}}^{(s)}}\sqrt{\xi^2 + \varepsilon}\right). \tag{7d}$$

The curves in Fig. 6 constructed using formulae (7) under the same conditions as in Fig. 5 ($b/a \approx 0.25$) show that the first DTR branch corresponding to an excited X-ray wave with the absorption coefficient $\mu_1^{(s)}$ contributes mainly to the spectral density. For this wave, the maxima of antinodes of the standing X-ray wave are in the layer with a small electron density; therefore, the decrease in the decay of its amplitude can be interpreted as the manifestation of the Borrmann effect in the DTR of relativistic electrons in the layered medium. The contribution of the second DTR branch is negligibly small, because its dynamic absorption coefficient is much higher than the kinematic one ($\mu_2^{(s)} > \mu_0$) (Fig. 4). The antinode maxima of the standing X-ray wave are located in the medium

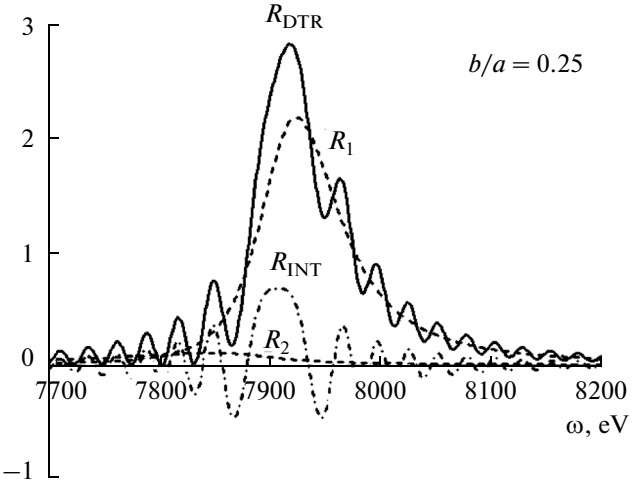

Fig. 6. Contribution of two branches of X-ray waves excited in the layered medium and of their interference in the DTR spectrum under the condition of Borrmann effect manifestation.

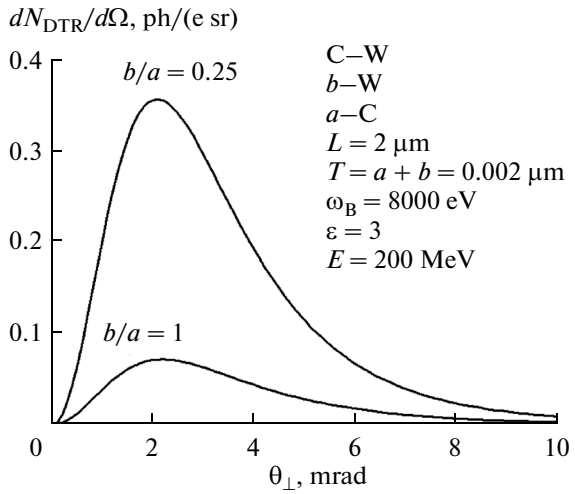

Fig. 7. Angular DTR density under the condition of clear manifestation of the Borrmann effect $b/a \approx 0.25$ and in the case $b/a \approx 1$.

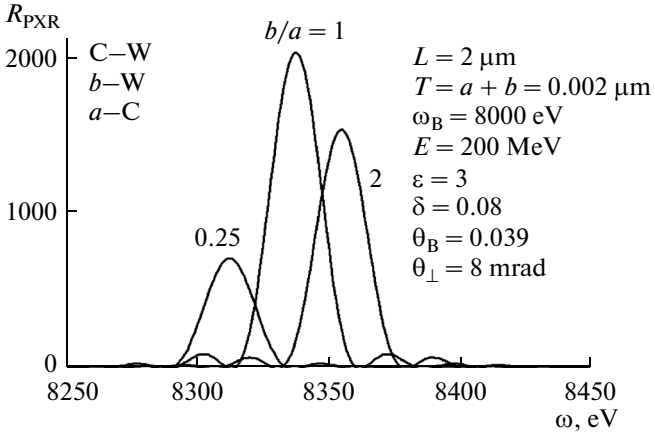

Fig. 8. PXR spectra for different ratios b/a of the target layer thicknesses.

layers in which the electron density is maximum. It is necessary to mention that, in spite of the negligibly small contribution of the second branch to the total spectral density, the interference $R^{(s)}_{INT}$ of the two DTR branches leads to noticeable oscillations in the frequency dependence of the total spectral radiation density (Fig. 6).

We consider the angular DTR densities for different ratios b/a of layer thicknesses. Figure 7 shows curves describing the angular DTR density constructed using formula (6). It can be seen that, as the ratio b/a decreases, the angular density increases significantly, because parameter $\kappa^{(s)}$ increases (Fig. 2), and the dynamic absorption coefficient $\mu_1^{(s)}$ decreases together with it, which determines the significant Borrmann effect in the angular DTR density.

We consider the influence of dynamic effects on the PXR of relativistic electrons in a layered medium. Analyzing expression (1), which describes the PXR spectrum, we can see that, unlike DTR, PXR forms in a layered medium by only one X-ray wave with the absorption coefficient $\mu_1^{(s)}$. We consider the spectrum in the case where there is no absorption; in this case, expression (1b) becomes

$$R^{(s)}_{PXR} = 4\left(1 - \frac{\xi^{(s)}(\omega)}{\sqrt{\xi^{(s)}(\omega)^2 + \varepsilon}}\right)^2 \times \frac{\sin^2\left(\frac{L_e}{4L_{ext}}\left(\sigma^{(s)} + \frac{\xi^{(s)}(\omega) - \sqrt{\xi^{(s)}(\omega)^2 + \varepsilon}}{\varepsilon}\right)\right)}{\left(\sigma^{(s)} + \frac{\xi^{(s)}(\omega) - \sqrt{\xi^2 + \varepsilon}}{\varepsilon}\right)^2}. \quad (8)$$

Curves describing the spectral PXR density of the relativistic electron for different values of the ratio b/a constructed using formula (8) are given in Fig. 8. As in the consideration of DTR, the electron energy $E =$ 200 MeV. It can be seen that, under the condition given in the figure, the spectrum with the maximum amplitude corresponds to $b/a \approx 1$. This is due to the fact that the denominator in (8) for this ratio has the minimal value. The closeness of the denominator in (8) to zero corresponds to the physical condition for the appearance of the PXR reflection in the case of which the real part of the wave vector of the pseudophoton of the relativistic-electron Coulomb field coincides with that of a free photon; i.e., in the case where the bound photon becomes free. The equality of the denominator in (8) to zero determines the frequency ω_*, in the area of which the spectrum of PXR photons emitted at a fixed observer angle is concentrated.

We consider the angular part of expression (1) for σ-polarized waves $(\theta_\perp = \theta\sin\varphi)$, it has the form

$$F_{PXR} = \frac{e^2}{4\pi^2} P^{(s)^2} \frac{\theta_\perp^2}{\left(\theta_\perp^2 + \gamma^{-2} - (\chi'_a + r\chi'_b)/(1+r)\right)^2}. \quad (9)$$

The curves constructed using formula (9) for the conditions in Fig. 8 and given in Fig. 9 show that the angular distribution of pseudophotons of the relativistic-electron Coulomb field has a larger amplitude for a smaller compound density. Because the W- and C layer thicknesses are determined by the parameters b and a, respectively, a smaller ratio b/a corresponds to a smaller average density of the medium for the fixed structure period $T = a + b$. Using formulae (8) and (1a), we construct curves (Fig. 10) describing the spectral and angular PXR densities for the observation angle $\theta_\perp$ corresponding to the angular-density maximum. It can be seen that the spectrum corresponding to the ratio $b/a \approx 1$ has the largest amplitude, although

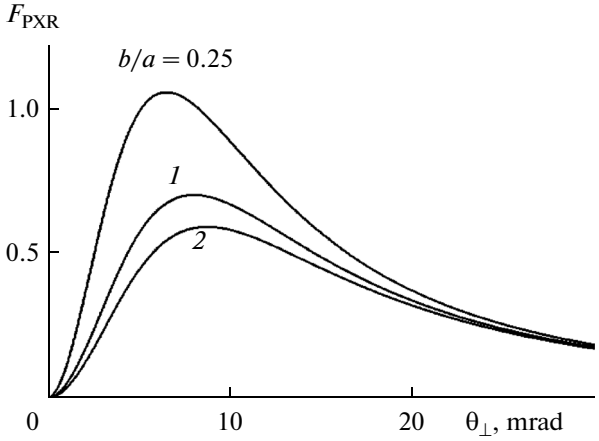

Fig. 9. Angular part of the spectral and angular PXR densities for different values of the ratio b/a.

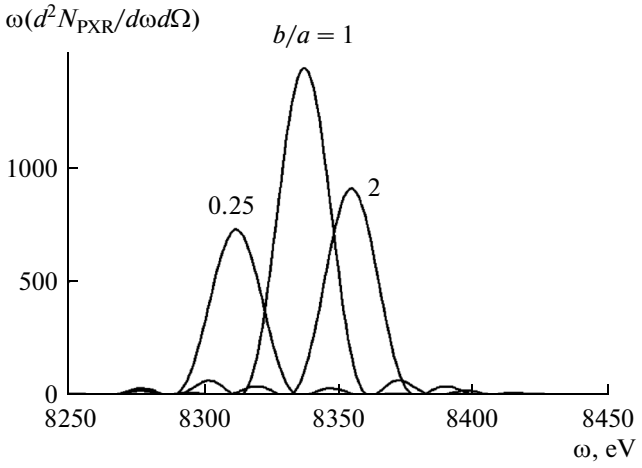

Fig. 10. Spectral and angular PXR densities for different ratios b/a. The parameters are the same as in Fig. 8.

the largest amplitude of the angular density corresponds to the parameter $b/a \approx 0.25$ (Fig. 9). We consider the spectral and angular PXR densities of the relativistic electron by taking the radiation-photon absorption of the layered medium into account. Figure 11 shows curves constructed using formula (1) under the conditions in Fig. 10, but taking photon absorption by the medium into account. It follows from comparison between Figs. 10 and 11 that, because of absorption, the amplitude of the PXR spectrum for the medium with the parameter $b/a \approx 1$ decreases more significantly than for the medium with the parameter $b/a \approx 0.25$. The small decrease in the amplitude in the case where absorption is taken into account means that the antinode maxima of the standing wave under the condition $b/a \approx 0.25$ are located in medium places where the electron density is minimal as in the case of DTR. Thus, the Borrmann effect is also manifested in the PXR of the relativistic electron in a periodic layered medium.

We consider the influence of the asymmetry of reflection of the relativistic-electron field (the parameter ε) with respect to the target surface determined by the angle δ between the reflecting layers and the target surface on the PXR characteristics. For this purpose, we consider expression (8) describing the PXR spectrum in the case where absorption is lacking. The curves describing the spectra of relativistic-electron PXR in a periodic layered medium for two different values of the parameter of reflection asymmetry ε, which are unambiguously related to the angle δ for the fixed angle θ_B. It is necessary to note that both curves are constructed for the same electron path $L_e = 49$ μm in the layered medium, but for different target thicknesses L. Figure 12 predicts the dynamic effect of the change in the spectral width as the asymmetry of the electron-field reflection changes with respect to the target surface, i.e., as the angle δ varies. For the fixed angleθ_B between the electron velocity vector and a system of parallel diffracting compound layers, the decrease in the angle [delta], i.e., decrease in the angle $\delta - \theta_B$ of particle incidence on the layered-structure surface, leads to a significant increase in the spectral width. Because the dependence of the real part of the difference between the lengths of the wave vectors of the real and virtual photons on the frequency is determined by the reflection asymmetry, the PXR spectral width also depends on the asymmetry.

It can be seen directly from formula (8) that spectral broadening occurs with increasing ε as a result of weakening of the dependence of the denominator in the expression for $R^{(s)}_{PXR}$ on $\xi^{(s)}(\omega)$. The increase in the spectral width leads to a significant increase in the angular PXR density, which is demonstrated by the curves in Fig. 13 constructed using formulae (5) and

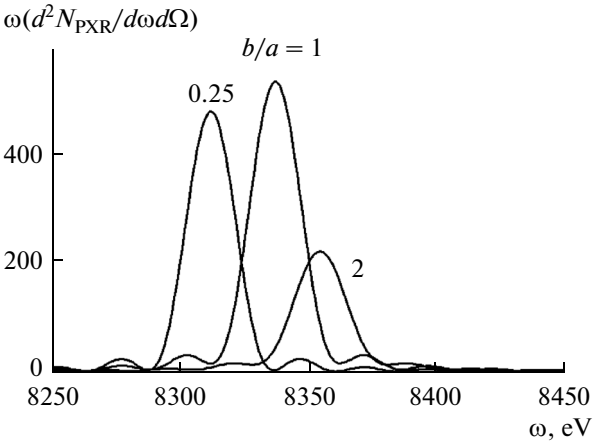

Fig. 11. Spectral and angular radiation densities for different ratios b/a in the case of an absorbing target.

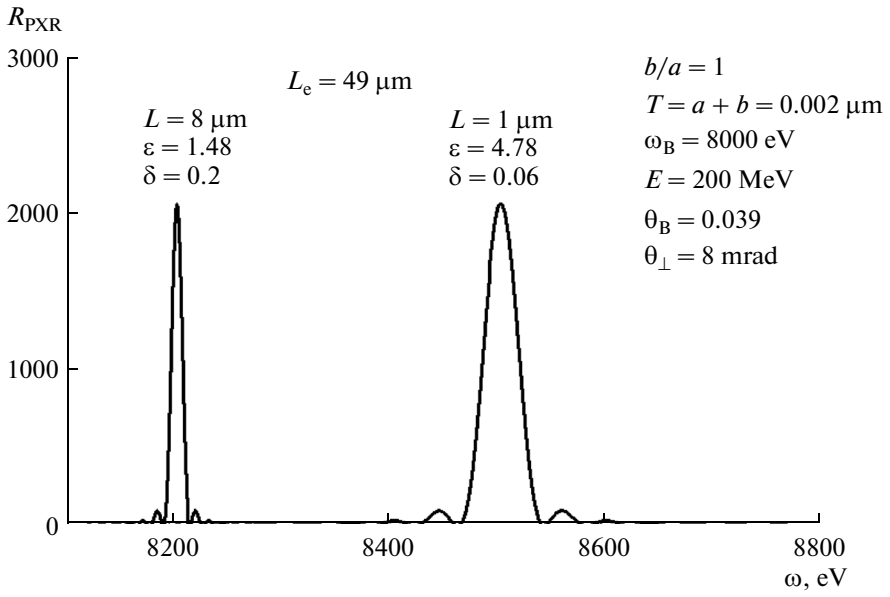

Fig. 12. Spectral PXR densities for two different values of the asymmetry parameter ε.

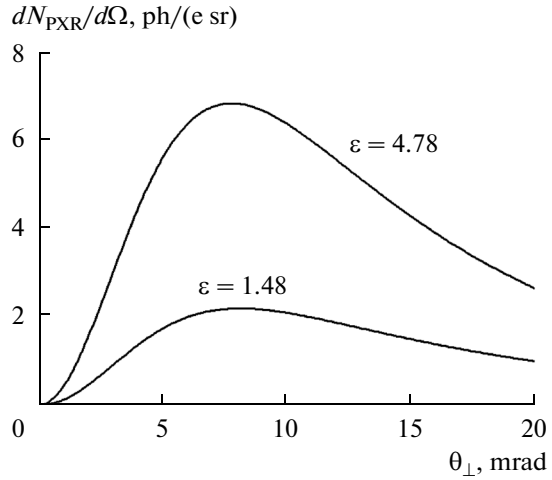

Fig. 13. Angular PXR densities for two different values of the asymmetry parameter ε.

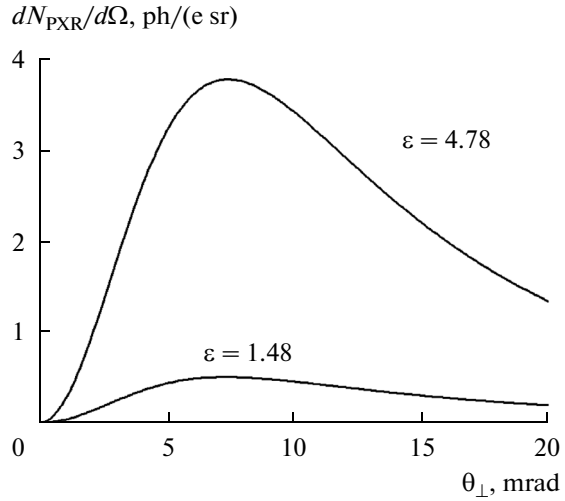

Fig. 14. Angular PXR densities for an absorbing target.

(8). If absorption is taken into account (Fig. 14), this effect is enhanced, because the length L_f of the maximum photon path in the layered medium increases with decreasing asymmetry parameter ε for a fixed length of the electron path in the target. The curves in Fig. 14 are constructed using formulae (5) and (1b).

CONCLUSIONS

In this paper, we have developed a theory of the effects of dynamic diffraction in he coherent X-ray radiation of relativistic electrons in a periodic layered medium. Based on the developed theory, we showed the possibility of manifestation of the effect of anomalously low photoabsorption (the Borrmann effect) in the DTR and PXR of relativistic electrons in a periodic layered medium. We showed that, if the ratio of the reflecting-layer thicknesses of different compounds is varied, then it is possible to obtain a condition for which the antinode maxima of the standing wave formed by superposition of the incident and reflected X-ray waves are located in layers with the smallest electron density where photoabsorption is minimal. Thus, there is the possibility of controlling the Borrmann effect in an artificial layered periodic medium.

Based on an expression obtained for the spectral and angular densities, we predicted and theoretically studied the dynamic effect of a variation in the spectral width of the relativistic-electron PXR in a periodic layered medium as the asymmetry of the particle-field reflection varies with respect to the target surface (the angle δ). We showed that, for a fixed angle between the electron velocity and a system of parallel diffracting atomic crystal planes (the Bragg angle θ_B), the decrease in the angle δ (decrease in the angle of particle incidence on the crystal surface $\delta - \theta_B$) leads to a significant increase in the spectral width and to a significant increase in the angular PXR density.

ACKNOWLEDGMENTS

The work was supported by the Russian Federation Ministry of Education and Sciences (project part of state task no. 3.500.2014/K in the sphere of scientific activity and state task no. 2014/420).

REFERENCES

1. M. L. Ter-Mikaelyan, *The Influence of the Medium on High-Energy Electromagnetic Processes* (AN ArmSSR, Yerevan, 1969) [in Russian].
2. M. L. Ter-Mikaelyan, Sov. Phys. Dokl. **5**, 1015 (1960).
3. F. R. Artutyunyan, K. A. Isparyan, and A. G. Oganesyan, Sov. J. Nucl. Phys. **1**, 604 (1965).
4. F. R. Artutyunyan and M. L. Ter-Mikaelyan, Usp. Fiz. Nauk **107**, 332 (1972).
5. V. L. Ginzburg and V. N. Tsytovich, Phys. Rep. **49**, 1 (1979).
6. M. L. Cherry and G. Hartmann, Phys. Rev. D: Part. Fields **10**, 3594 (1974).
7. X. Artu, G. Yodh, and G. Mennessier, Phys. Rev. D: Part. Fields **12**, 1289 (1975).
8. M. Deutschmann, et al., Nucl. Instrum. Methods Phys. Res. B **180**, 409 (1981).
9. C. W. Fabjan and W. Struczinski, Phys. Lett. B **57**, 483 (1975).
10. T. Tanaka et al., Nucl. Instrum. Methods Phys. Res. B **93**, 21 (1994).
11. K. Yamada, T. Hosokawa, and H. Takenaka, Phys. Rev. A **59**, 3673 (1999).
12. S. Asano, et al., Phys. Rev. Lett. **70**, 3247 (1993).
13. B. Pardo and J.-M. Andre, Phys. Rev. E **65**, 036501 (2002).
14. N. Zhevago, in *Proceedings of the 2nd Symposium on Transition Radiation of High Energy Particles, Yerevan, Armenia, 1983*, p. 200.
15. C. T. Law and A. E. Kaplan, Opt. Lett. **12**, 900 (1987).
16. B. Pardo and J.-M. Andre, Phys. Rev. A **40**, 1918 (1989).
17. M. S. Dubovikov, Phys. Rev. A **50**, 2068 (1994).
18. J.-M. Andre, B. Pardo, and C. Bonnelle, Phys. Rev. E **60**, 968 (1998).
19. B. Lastdrager, A. Tip, and J. Verhoevan, Phys. Rev. E **61**, 5767 (2000).
20. N. K. Zhevago and V. I. Glebov, Phys. Lett. A **309**, 311 (2003).
21. N. N. Nasonov, V. V. Kaplin, S. R. Uglov, M. A. Piestrup, and C. K. Gary, Phys. Rev. E **68**, 3604 (2003).
22. V. V. Kaplin, S. R. Uglov, V. N. Zabaev, M. A. Piestrup, C. K. Gary, N. N. Nasonov, and M. K. Fuller, Appl. Phys. Lett. **76**, 3647 (2000).
23. S. V. Blazhevich, I. V. Kolosova, and A. V. Noskov, J. Exp. Theor. Phys. **114**, 547 (2012).
24. S. V. Blazhevich, Yu. P. Gladkikh, and A. V. Noskov, J. Surf. Invest.: X-ray, Synchrotron Neutron Tech. **7**, 388 (2013).
25. S. Blazhevich, I. Kolosova, and A. Noskov, J. Phys.: Conf. Ser. **357**, 012016 (2012).
26. Z. G. Pinsker, *Dynamical Scattering of X-Rays in Perfect Crystals* (Nauka, Moscow, 1974) [in Russian].
27. N. Nasonov and A. Noskov, Nucl. Instrum. Methods Phys. Res. B **201**, 67 (2003).
28. S. V. Blazhevich and A. V. Noskov, Nucl. Instrum. Methods Phys. Res. B **266**, 3770 (2008).
29. S. V. Blazhevich and A. V. Noskov, Nucl. Instrum. Methods Phys. Res. B **266**, 3777 (2008).
30. S. V. Blazhevich and A. V. Noskov, J. Exp. Theor. Phys. **109**, 901 (2009).
31. S. V. Blazhevich and A. V. Noskov, J. Surf. Invest.: X-ray, Synchrotron Neutron Tech. **4**, 303 (2010).

Translated by L. Kul'man